



Title	Diffusion Bonding of Titanium Aluminide and Low-Carbon Steel Using a Spark Plasma Sintering System
Author(s)	Kohama, Kazuyuki; Ito, Kazuhiro
Citation	Transactions of JWRI. 2015, 44(2), p. 23-26
Version Type	VoR
URL	https://doi.org/10.18910/57273
rights	
Note	

The University of Osaka Institutional Knowledge Archive : OUKA

<https://ir.library.osaka-u.ac.jp/>

The University of Osaka

Diffusion Bonding of Titanium Aluminide and Low-Carbon Steel Using a Spark Plasma Sintering System[†]

KOHAMA Kazuyuki * and ITO Kazuhiro **

Abstract

Diffusion bonding of titanium-aluminide based alloys (TiAl) and SS400 low-carbon steels was conducted at 600 – 800°C for 0 – 60 min using a spark plasma sintering (SPS) system, then bonding strength of the TiAl/SS400 joints were evaluated by shear tests. Compared to previous studies regarding diffusion bonding of TiAl and high-carbon steels, the TiAl/SS400 joints exhibited considerably higher bonding strength. The reason for this is presumably based on increase in bonding area and formation of thinner TiC-based layers at the bonding interface derived from the higher deformability and lower carbon content in SS400. In addition, Vickers hardness measured on the surface of the TiAl and SS400 samples significantly increased after bonding regardless of the bonding temperature, showing that TiAl/SS400 joints with high surface hardness can be fabricated using the SPS system.

KEY WORDS: (TiAl), (SS400), (Bonding Interface), (Shear Strength), (Surface Hardening)

1. Introduction

Titanium-aluminide based alloys (hereafter referred to as “TiAl”), which in many cases consist of γ -TiAl + α_2 -Ti₃Al intermetallic compounds, exhibit superior physical properties such as light weight, high-temperature strength and resistance against oxidation. Due to the properties, TiAl is proposed as the alternative material for Ni-based superalloys used as turbine impellers in automotive and aircraft engines¹⁻⁵. Practical applications of the TiAl products requires reliable joining to structural steels such as shafts, and diffusion bonding is a proper joining method for these materials compared to other methods such as brazing and friction welding in terms of precision bonding and high-temperature reliability of the joints⁶⁻¹⁰. There have been some investigations on diffusion bonding of TiAl and steels¹¹⁻¹⁴, which reveal that bonding strength of the diffusion bonded TiAl/steel joints is likely to be degraded by the formation of TiC-based brittle layers with thicknesses of more than about 10 μ m at the bonding interface. Thus, reducing carbon content in the steels is recognized as one of the possible ways to obtain high-strength TiAl/steel joints by inhibiting the interfacial TiC formation. In this study, diffusion bonding of TiAl and SS400 low-carbon steel samples was conducted using a spark plasma sintering (SPS) system, which is currently emerging as a diffusion bonding method for many bulk materials¹⁵⁻²⁰.

Dependence of the bonding strength on microstructure of the bonding interface for the TiAl/SS400 joints was fundamentally investigated. Also, surface hardness of the joints was evaluated by Vickers hardness tests because the sample surface was expected to be hardened during bonding due to exposure to graphite vapor generated from the heated graphite fixtures.

2. Experimental procedure

The materials used in this study were TiAl (54.3at.%Ti -41.1at.%Al -2.2at.%Cr -2.4at.%Nb) and SS400 low-carbon steel (0.17wt.%C -0.02wt.%Si -0.50wt.%Mn -0.009wt.%P -0.006wt.%S -bal. Fe) plates. These were cut into small rectangular samples with dimensions of 4 × 5 × 6 mm³. The bottom (4 × 5 mm²) and side (5 × 6 mm²) surface of the samples were polished using diamond lapping films for bonding and Vickers hardness tests, respectively, and then ultrasonically cleaned with acetone. Diffusion bonding of the TiAl and SS400 samples was conducted using an SPS system. **Figure 1** shows a schematic illustration of the sample position arranged in the SPS chamber. The samples were directly touched together and held between upper and lower graphite punches in a cylindrical graphite die. A carbon sheet was placed between the sample and punch for impact absorption and prevention

[†] Received on December 18, 2015

* Assistant Professor

** Professor

Diffusion Bonding of Titanium Aluminide and Low-Carbon Steel Using a Spark Plasma Sintering System

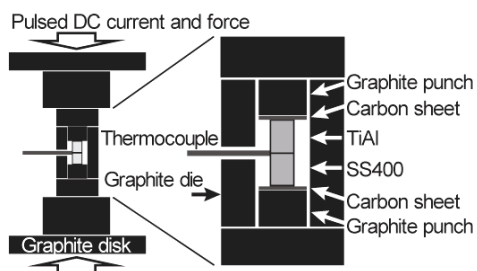


Fig. 1 A schematic illustration for position of TiAl and SS400 samples arranged in the SPS system.

of reaction. The top surface of the upper punch flushed with that of the die, and thus compressive stress was not initially applied to the samples but gradually increased with increasing temperature due to thermal expansion difference between graphite and the samples. Prior to the heating process, vacuum pressure in the SPS chamber was about 20 Pa. Then, the samples were heated by applying a pulsed DC current to both the graphite fixtures and samples. The bonding temperature was directly measured using a K-type thermocouple installed through the hole in the graphite die, and varied from 600°C to 800°C. The heating rate was 100°C/min from room temperature (RT) to the bonding temperature. The holding time at the bonding temperature was 0 – 60 min. After the bonding process, the samples were cooled down to less than ~150°C in vacuum. Bonding strength of the TiAl/SS400 joints was evaluated by shear tests. The crosshead speed was set to 0.1 mm/min. Cross-sectional microstructure around the bonding interface was observed using a scanning electron microscope (SEM) equipped with an energy dispersion x-ray (EDX) spectroscopy system. The Vickers hardness tests used a square-based diamond pyramid with a 136° point angle. The applied force was varied from 0.03 to 0.5 kgf, and force-maintaining time was 15 s. Note that no additional treatments other than cleaning with acetone were performed on the measurement surface before and after bonding.

3. Results and Discussion

3.1 Appearance of the TiAl/SS400 joints

The TiAl and SS400 samples were successfully bonded at 600 – 800°C for 0 – 60 min. **Figure 2** shows appearance of the TiAl/SS400 joint bonded at 600°C for 20 min. All the other joints had similar appearance, and no severe defects such as cracks at the interface were observed.

3.2 Shear test results for the TiAl/SS400 joints

In order to evaluate bonding strength of the joints, shear tests were conducted. The applied shear stress increased proportionally with increasing the displacement and reached the maximum value, i.e. shear fracture stress, at which all the joints failed at the bonding interface. As shown in **Fig. 3**, the shear fracture stress for the joints

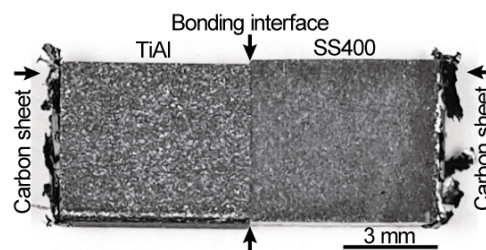


Fig. 2 Appearance of the TiAl/SS400 joint bonded at 600°C for 20 min.

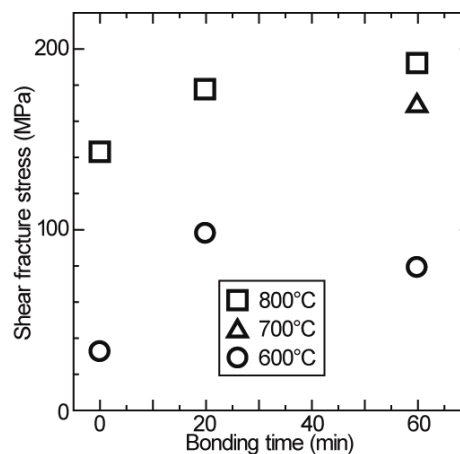


Fig. 3 Dependence of shear fracture stress on bonding temperature and time for the TiAl/SS400 joints.

tended to increase with increasing the bonding time and temperature. This suggests that elemental intermixing and/or void shrinkage at the bonding interface were enhanced as the time and temperature increased. The joints bonded at 600 and 700°C showed considerably high shear fracture stress, whereas no successful diffusion bonding of TiAl and high-carbon steels at less than 800°C has been reported in previous studies¹²⁻¹⁴. In addition, the shear fracture stress for the joints bonded at 700 and 800°C were found to be higher than those for the joints bonded at 600°C.

3.3 Cross-sectional SEM observation around the bonding interface

To investigate the relationship between the mechanical properties and cross-sectional microstructure around the bonding interface for the TiAl/SS400 joints, SEM and EDX analyses were carried out. As seen in **Fig. 4(a)**, there are several voids remaining at the interface for the joints bonded at 600°C for 60 min. In addition, elemental line profiles obtained across the bonding interface along L1 show no distinct segregation nor chemical reaction at the interface (**Fig. 4(c)**). These results suggest that the diffusion bonding of TiAl and SS400 at lower temperature was dominantly controlled by interfacial void shrinkage and mutual diffusion. As the temperature increased to 700°C, the number of interfacial

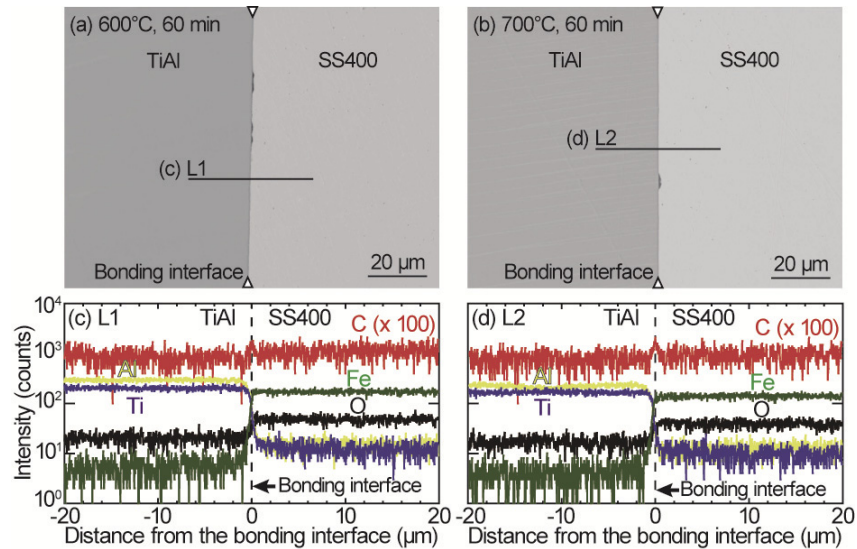


Fig.4 Cross-sectional SEM images around the bonding interface for the TiAl/SS400 joints bonded at (a) 600°C and (b) 700°C, for 60 min, and corresponding elemental line profiles across the bonding interface along (c) L1 and (d) L2, respectively.

voids were reduced, which resulted in the increased bonding area (**Fig. 4(b)**). In addition, C atoms were found to segregate at the interface (**Fig. 4(d)**), suggesting formation of a very thin TiC-based layer by diffusion reaction. Based on these results, the higher shear strength for the TiAl/SS400 joints bonded at 600°C attributed to higher deformability of SS400 compared to high-carbon steels, while the much higher shear strength for the TiAl/SS400 joints bonded at 700 and 800°C can be explained by combination of the increased bonding area and the formation of vary thin TiC-based layers at the interface.

3.4 Vickers hardness for the TiAl/SS400 joints

Figure 5 shows Vickers hardness measured on the surface of the TiAl and SS400 samples before and after bonding, plotted as a function of the applied force. Note that the larger force corresponds to the larger indentation depth from the sample surface. As shown in **Fig. 5(a)**, the SS400 sample before bonding exhibited almost constant hardness values of about 120 Hv regardless of the applied force, indicating homogeneous microstructure and

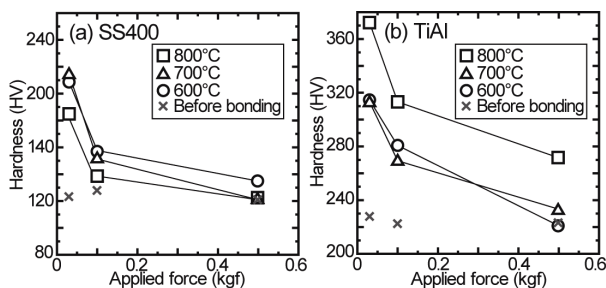


Fig. 5 Vickers hardness measured on the surface of the (a) SS400 and (b) TiAl samples before and after bonding using the SPS system, plotted as a function of the applied force.

hardness in the sample. In contrast, the values obviously increased after bonding at 600 – 800°C for 60 min, and the increments depended on the applied force: the larger hardness values were obtained for the lower applied force. This indicates that the hardness near the sample surface were larger than those inside the samples. Similar surface hardening behavior was obtained for the TiAl samples (**Fig. 5(b)**). We concluded that the surface of the TiAl and SS400 samples were hardened during bonding due to exposure to the graphite vapor, although further investigation of dependence of the surface hardening behavior on bonding temperature and time is needed.

4. Summary

TiAl and SS400 samples were directly diffusion bonded using the SPS system, then shear strength and surface hardness for the TiAl/SS400 joints were evaluated. The samples were successfully bonded at 600 – 800°C for 0 – 60 min with no severe defects such as cracks at the bonding interface. The shear fracture stress for the joints increased with increasing the bonding temperature and time, and exhibited the maximum values of about 100, 170 and 200 MPa for the joints bonded at 600, 700 and 800°C, respectively. The values for the joints bonded at 600 and 700°C were considerably high, considering that no successful diffusion bonding of TiAl and high-carbon steels at less than 800°C has been reported in previous studies. SEM/EDX observations around the bonding interface revealed that the interfacial void shrinkage, as well as mutual diffusion, controlled the diffusion bonding, suggesting that higher deformability of low-carbon steels compared to high-carbon steels contributed to the low-temperature bonding. In addition, the formation of very thin TiC-based layers at the bonding interface for the joints bonded at 700°C and

Diffusion Bonding of Titanium Aluminide and Low-Carbon Steel Using a Spark Plasma Sintering System

higher increased the bonding strength to much higher. Vickers hardness tests showed that hardness near the sample surface were larger than those inside the samples regardless of the bonding temperature, showing that TiAl/SS400 joints with high surface hardness can be fabricated using the SPS system.

Acknowledgements

The authors would like to thank Masayoshi Kamai, Joining and Welding Research Institute, Osaka University, for his help in the SPS work.

References

- ¹ P. Bartolotta, J. Barrett, T. Kelly, and R. Smashey, *JOM* **49**, 48 (1997).
- ² J. Lapin, 18th International Metallurgical & Materials Conference Proceedings, 77 (2009).
- ³ T. Noda, *Intermetallics* **6**, 709 (1998).
- ⁴ T. Tetsui, *Curr. Opin. Solid State Mater. Sci.* **4**, 243 (1999).
- ⁵ T. Tetsui, M. Kyoya, and Y. Miura, *Mitsubishi Heavy Ind. Ltd. Tech. Rev.* **37**, 88 (2000).
- ⁶ J. Cao, J. Qi, X. Song, and J. Feng, *Materials* **2014**, 4930 (2014).
- ⁷ W. B. Lee, M. G. Kim, J. M. Koo, K. K. Kim, D. J. Quesnel, Y. J. Kim, and S. B. Jung, *J. Mater. Sci.* **39**, 1125 (2004).
- ⁸ W. B. Lee, Y. J. Kim, and S. B. Jung, *Intermetallics* **12**, 671 (2004).
- ⁹ Y. Li, P. He, and J. Feng, *Scr. Mater.* **55**, 171 (2006).
- ¹⁰ T. Noda, T. Shimizu, M. Okabe, and T. Iikubo, *Mater. Sci. Eng. A* **239-240**, 613 (1997).
- ¹¹ P. He, J.C. Feng, and W. Xu, *Mater. Sci. Eng. A* **418**, 45 (2006).
- ¹² P. He, J.C. Feng, B. G. Zhang, and Y. Y. Qian, *Mater. Charact.* **50**, 87 (2003).
- ¹³ P. He, J. Feng, B. Zhang, and Y. Qian, *Mater. Charact.* **48**, 401 (2002).
- ¹⁴ Y. Morizono, M. Nishida, A. Chiba, T. Yamamuro, Y. Kanamori, and T. Terai, *Mater. Trans.* **45**, 527 (2004).
- ¹⁵ A. Stern, I. Rosenthal, R. Aroshas, S. Kalabukhov, M. P. Dariel, and N. Frage, *Ann. "DUNAREA JOS" Univ. GALATI Fascicle XII Weld. Equip. Technol.* **23**, 5 (2012).
- ¹⁶ A. Allemand and F. Audubert: 'Process for Joining Refractory Ceramic Parts by Spark Plasma Sintering (SPS)', US Patent 0139840, published 10 June 2010.
- ¹⁷ B. Mouawad, M. Soueidan, D. Fabrègue, C. Buttay, V. Bley, and B. Allard, *Adv. Mater. Res.* **324**, 177 (2011).
- ¹⁸ B. Mouawad, M. Soueidan, D. Fabregue, C. Buttay, B. Allard, V. Bley, H. Morel, and C. Martin, *IEEE Trans. Compon. Packag. Manuf. Technol.* **2**, 553 (2012).
- ¹⁹ A. Miriyev, A. Stern, E. Tuval, S. Kalabukhov, Z. Hooper, and N. Frage, *J. Mater. Process. Technol.* **213**, 161 (2013).
- ²⁰ J. Yang, J. Trapp, Q. Guo, and B. Kieback, *Mater. Des.* **52**, 179 (2013).